Table 2
Basic rotor parameters

Rated wind speed, U_0	Tip diameter	Hub diameter	Tip speed ratio λ	Number of blades	Airfoil
5.7 m s^{-1}	0.91 m	0.25 m	5	6	SD2030

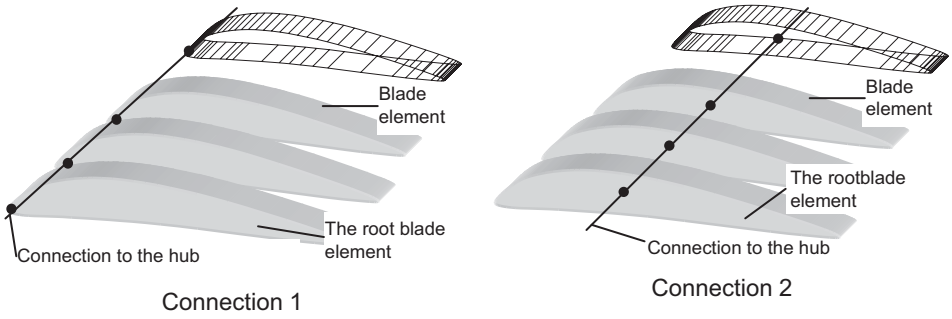


Fig. 9. Schematic diagram of connecting the blade elements together to form a blade and attachment of the blade onto the hub.

literature. There are for a Reynolds number for aeroplanes that is much higher than that for small wind turbines in a built environment.

Having defined geometric details for each of the blade elements, the connection of these elements together to form the blade and attach to the hub were to be decided. Two connection methods (CM) were applied for the blade elements and then joining with the hub: connecting each leading edge of the elements together and then attach the leading edge of the root element into the hub (noted as CM = 1 in Table 1); or connecting the elements along a straight line or curve by passing the middle points of each chord of the blade elements (CM = 2). The two rotor using the two connection methods were modelled again in the virtual wind tunnel and the criterion was the efficiency of power output, although other aspects were also taken into considerations: such as the structure strength; dynamics characteristics of the rotor as whole; aesthetics; aeroacoustic noise; and cost of manufacture. Fig. 9 illustrates the two methods of connecting all the blade elements and the hub (Option 1 and 2) whilst Table 1 (last column) lists the estimated power output. The calculated figures indicate that Option 2 could produce more power than Option 1. So connection method 2 was used to model the blades in the next six tests carried out thereafter.

3.2. Nose cone and nacelle design

Among the four profiles of the nose cone and nacelle in Table 1 (Options 3–6, respectively), the profile in Option 6 was found able to generate the maximum power. Hence Option 6 was compared further with its shorter version Option 7, and the results revealed that the shorter version was better in terms of power yield. Along with the common sense that the diameter of the nose and nacelle should be as small as possible, this finding suggests that the volume of the nose cone and nacelle should be kept as small as possible to achieve the best performance. However, the space created by the nose and nacelle needs to accommodate the generator, which would prefer bigger to be more efficient in producing electricity. Therefore there lies a trade-off between the aerodynamics and electricity to achieve the optimal performance for the rotor as whole.

In Table 1, two design options (Options 7 and 8) which are describing the different position of rotor in the scoop were computed in the virtual wind tunnel. According to the previous computations [18], the maximum acceleration speed ratio was found at the position 0.6 m away from the inlet of the scoop. From the computation for the rotor in the scoop, the free stream wind was blocked by the existence of the rotor, which changed the wind speed distribution along the scoop. For this reason, the position of the rotor in the scoop should be optimised according to different position. The results suggest that the position to achieve the better performance should be located near the inlet of the scoop rather than the maximum speed up position without scoop.

3.3. The predicted flow fields

As the CFD model calculated for all the flow variables, such as the pressure, the velocity components, and turbulent features over 100,000 points, selecting various could help to understand more about the flow field.

Fig. 10(a) shows a rather evenly distributed surface pressure on the pressure side of the rotor. This was achieved by twisting the blade gradually more towards the tip. The actual difference was just over 2.1 Pa between the root and the tip. But on the suction side, the difference was much bigger: the pressure was over 30 Pa lower at the tip than the root (Fig. 10(b)). Therefore the pressure difference between the two sides at a section increased towards the tip

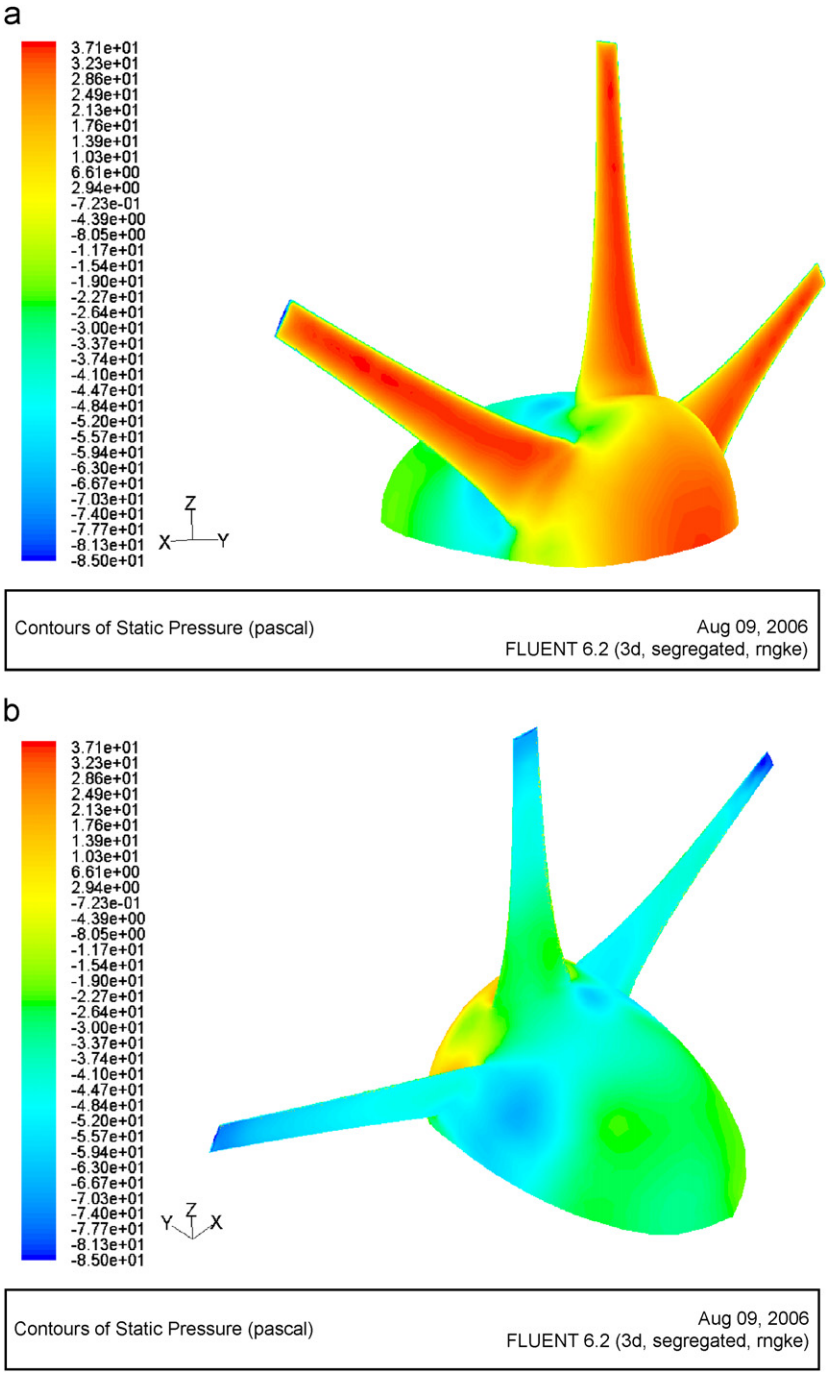


Fig. 10. The pressure distribution over the rotor surfaces. (a) The pressure side, (b) the suction side.

of each blade. Even as the chord decreased, the production of the surface area and pressure, the force that drove the blade rotating could remain still be strong at the tip than at the root of a blade. When torque is considered, the most important part of a rotor then would be the tip.

In Fig. 11, the air flow around the root (a) and tip (b) of the blade is projected on to two cross-section planes. These two plots were assumed moving with the rotating blade. As expected, they show geometrically the airfoil with the longer chord and the more twisted angle at the root than the one at the tip. Graphically the longer arrows around the tip on the plots indicate that the incoming wind was faster at the tip than that at the root. The two plots also suggest that the flow was much slower at the centre than the edge. This suggests the stronger flow near the tips of blades would be very beneficial as the flow drives the blade with a longer moment arm. The two effects resulted in much larger torque to rotate the rotor.

A closer look also reveals that the flow around the tip of the blades, split into two streams almost at the middle of the chord and formed two smaller vortexes about similar size behind the suction surface of the blade,

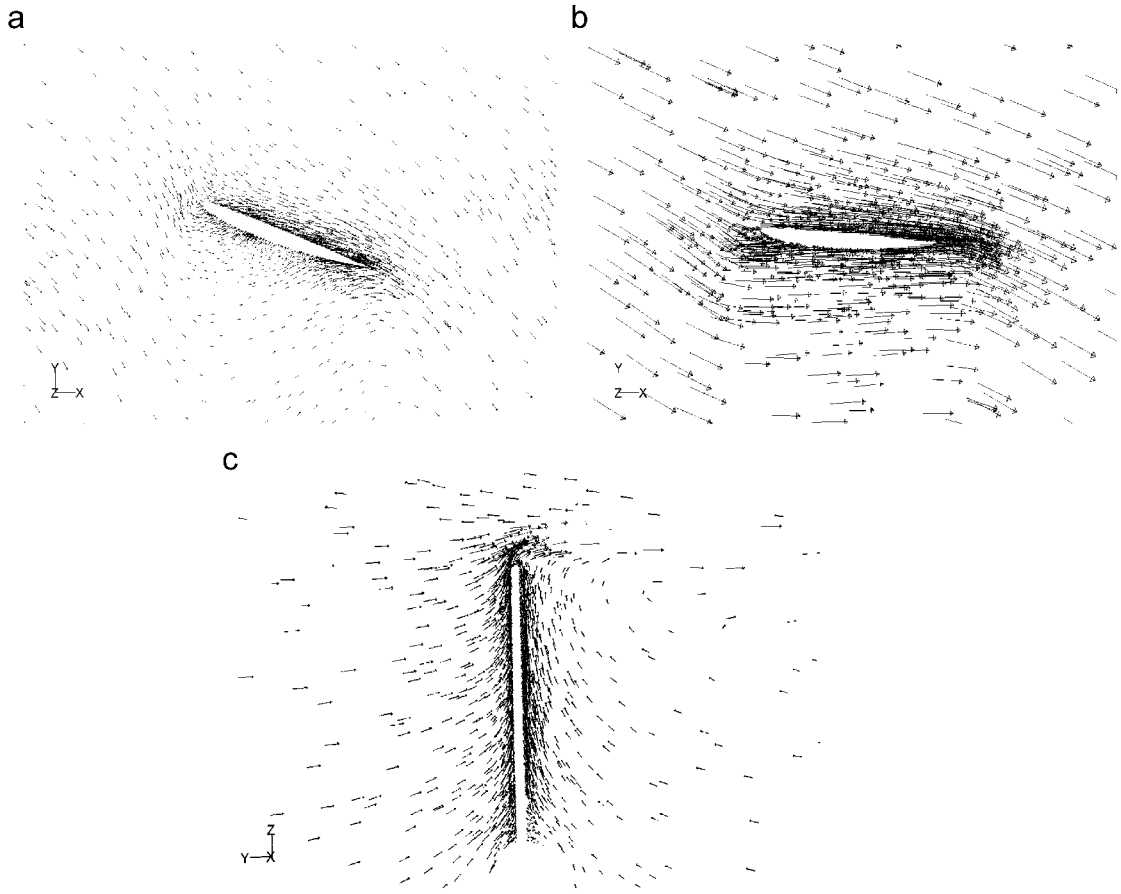


Fig. 11. Flow details shown by vectors on two planes across the chord of the blade. (a) On the across section near the root of the blade. (b) On the across section near the tip of the blade. (c) Flow around the blade, the cross section parallel to longitudinal direction of the blade.

whilst the separation at the root was closer towards the leading edge of the chord and the flow over the leading edge created a larger vortex than the other flow over the trailing edge. The plots of pressure contours also indicate that the pressure difference between the pressure and suction surface was higher on the tip than on the root (Fig. 12). Moreover, the lever arm of the tip was also much larger than that at the root. Hence the torque generated at the tip was much larger than that at the root, which was considered to be the major contributor for higher energy generation. This explanation agrees well with the physical analysis [25].

Fig. 11(c) shows the flow details along the radial direction of the rotor: flow diverting towards to the tip, or the gap between the scoop and the rotor. It shows that the air flow tended to move outwards along the disk radius because of the centrifugal effect. This phenomenon is also referred as the pump effect in the rotating cavity flow. Moreover, the longitudinal flow component is much stronger due to two reasons, firstly the blockage of the existence of the turbine, and secondly the acceleration near the inner surface of the scoop. The latter could require a high twist angle that calculated here using the BEM method without taking into account of uneven distribution of incoming flow induced by the scoop acceleration.

3.4. Power curve and annual power output

Comparison on the power curve between the tested wind turbine with the other three in similar swept area shows that the test one was better than the two of exact same swept area and very close to WS1000, which is 36% larger in the swept area (Fig. 13(a)). Therefore the tested wind turbine would perform rather well in terms of power yield (Table 3) .

A close look at these curves shows that at the low speeds, the tested turbine did not produce more power than others(Fig. 13(b)). This was rather unexpected as the scoop did boost the airflow inside. The power generation was only starting to be better than the other two same size turbines after about $6.5\,m\,s^{-1}$, a figure normally higher than the most frequent occurring winds at most built areas.

It is worth of mentioning that the power curve is also readily available from the Fortune code developed to calculate the blade's parameters. But because those two coefficients were derived from high Reynolds number flows, it was considered better to rely on the methods using the predicted pressures by the CFD model

Prediction of power yield over a year seems encouraging. Using the actual wind data, the tested wind turbine could produce 872 kWh, more than other wind turbines of same